Received: 23 May 2020 | Revised: 1 September 2020 | Accepted: 11 September 2020

DOI: 10.1096/fj.202001258RR

RESEARCH ARTICLE

THE FASEB JOURNAL

Thyroid hormone receptor α in skeletal muscle is essential for T3-mediated increase in energy expenditure

Trine S. Nicolaisen[1,2] | Anders B. Klein[1] | Oksana Dmytriyeva[1,3] | Jens Lund[1] | Lars R. Ingerslev[1] | Andreas M. Fritzen[2] | Christian S. Carl[2] | Anne-Marie Lundsgaard[2] | Mikkel Frost[1] | Tao Ma[1] | Peter Schjerling[4] | Zachary Gerhart-Hines[1] | Frederic Flamant[5] | Karine Gauthier[5] | Steen Larsen[6] | Erik A. Richter[2] | Bente Kiens[2] | Christoffer Clemmensen[1]

[1]Novo Nordisk Foundation Center for Basic Metabolic Research, Faculty of Health and Medical Sciences, University of Copenhagen, Copenhagen, Denmark

[2]Section of Molecular Physiology, Department of Nutrition, Exercise and Sports, Faculty of Science, University of Copenhagen, Copenhagen, Denmark

[3]Department of Biomedical Sciences, Faculty of Health and Medical Sciences, University of Copenhagen, Copenhagen, Denmark

[4]Institute of Sports Medicine Copenhagen, Department of Orthopedic Surgery, Bispebjerg-Frederiksberg Hospital and Center for Healthy Aging, Faculty of Health and Medical Sciences, University of Copenhagen, Copenhagen, Denmark

[5]Institut de Génomique Fonctionnelle de Lyon, Université de Lyon, Université Lyon 1, CNRS UMR 5242, INRA USC 1370, Ecole Normale Supérieure de Lyon, Lyon, France

[6]Xlab, Center for Healthy Aging, Department of Biomedical Sciences, Faculty of Health and Medical Sciences, University of Copenhagen, Copenhagen, Denmark

Correspondence
Christoffer Clemmensen, Novo Nordisk Foundation Center for Basic Metabolic Research, Faculty of Health and Medical Sciences, University of Copenhagen, Blegdamsvej 3B, 2200-Copenhagen, Denmark.
Email: chc@sund.ku.dk

Funding information
Novo Nordisk Fonden (NNF), Grant/Award Number: NNF17SA0031406, NNF17OC0026114 and NNF18CC0034900; Alfred Benzon Foundation; Danish Council for Independent Research, Grant/Award Number: 7016-00389A; Lundbeck Foundation, Grant/Award Number: R238-2016-2859; University of Copenhagen

Abstract

Thyroid hormones are important for homeostatic control of energy metabolism and body temperature. Although skeletal muscle is considered a key site for thyroid action, the contribution of thyroid hormone receptor signaling in muscle to whole-body energy metabolism and body temperature has not been resolved. Here, we show that T3-induced increase in energy expenditure requires thyroid hormone receptor alpha 1 ($TR\alpha_1$) in skeletal muscle, but that T3-mediated elevation in body temperature is achieved in the absence of muscle-$TR\alpha_1$. In slow-twitch soleus muscle, loss-of-function of $TR\alpha_1$ ($TR\alpha^{HSACre}$) alters the fiber-type composition toward a more oxidative phenotype. The change in fiber-type composition, however, does not influence the running capacity or motivation to run. RNA-sequencing of soleus muscle from WT mice and $TR\alpha^{HSACre}$ mice revealed differentiated transcriptional regulation of genes associated with muscle thermogenesis, such as sarcolipin and UCP3, providing molecular clues pertaining to the mechanistic underpinnings of $TR\alpha_1$-linked control

Abbreviations: AMPK, AMP-activated kinase; BAT, brown adipose tissue; DIO, diet-induced obesity; DIO2, deiodinase type 2; EDL, extensor digitorum longus; GDF15, growth differentiation factor 15; HFD, high-fat diet; iWAT, inguinal white adipose tissue; KO, knock-out; s.c., subcutaneously; SNS, sympathetic nervous system; SOL, soleus; T3, triiodothyronine; T4, thyroxine; $TR\alpha_1$, thyroid hormone receptor alpha 1; UCP1, uncoupling protein 1; WT, wild-type.

Trine S. Nicolaisen and Anders B. Klein are Co-first author.

of whole-body metabolic rate. Together, this work establishes a fundamental role for skeletal muscle in T3-stimulated increase in whole-body energy expenditure.

KEYWORDS

energy expenditure, energy metabolism, skeletal muscle, thyroid hormone

1 | INTRODUCTION

Thyroid hormones (triiodothyronine (T3) and thyroxine (T4)) influence a multitude of physiological functions mirrored by the ubiquitous expression of thyroid hormone receptors throughout the body.[1] Notably, excess thyroid hormone production (hyperthyroidism) or administration of exogenous thyroid hormone potently increases the energy metabolism.[1] Cumulative evidence underscores that this endocrine effect, sometimes referred to as "thyroid thermogenesis," involves both central and peripheral mechanisms of action.[1] In context, thyroid hormone-induced stimulation of muscle and liver Na^+/K^+ ATPase activity, as well as induction of futile cycling of Ca^{2+} between cytoplasm and sarcoplasmic reticulum in muscle, has undergone considerable scientific scrutiny.[2] Sympathetic nervous system (SNS)-induced brown adipose tissue (BAT) non-shivering thermogenesis has also been linked to thyroid thermogenesis.[2] Activation of the SNS induces the expression of the enzyme deiodinase type 2 (DIO2), which facilitates the conversion of T4 to T3 that, in turn, increases the expression of uncoupling protein 1 (UCP1) in BAT.[3,4] Furthermore, central T3 actions activate BAT thermogenesis via an AMP-activated kinase (AMPK)-dependent mechanism in the hypothalamus, emphasizing the importance of BAT as a primary site for thyroid thermogenesis.[5]

Surprisingly, two independent investigations recently reported that BAT thermogenesis is dispensable for thyroid hormone-induced increase in energy expenditure.[6,7] It was reported that although thyroid hormones increase UCP1 in BAT and induce browning of inguinal white adipose tissue (iWAT), these changes do not translate to an increased metabolic rate. In fact, thyroid hormone-induced increases in energy expenditure, body temperature, and food intake were similar between UCP1 knock-out (KO) and wild-type (WT) mice.[7] While Dittner and colleagues[7] speculated that thyroid hormone-mediated increase in energy expenditure might be secondary to thyroid hormone-induced elevation in body temperature governed by the brain, Johann et al,[6] hypothesized that stimulation of the thyroid hormone receptor alpha 1 ($TR\alpha_1$) in slow-twitch muscle contributes to T3-associated hyperthermia.

In skeletal muscle, $TR\alpha_1$ is the primary receptor,[8] and to resolve whether thyroid hormone action in muscle is necessary for thyroid hormone-mediated increase in energy expenditure and the associated increase in body temperature, we developed a skeletal muscle-specific $TR\alpha_1$-dominant negative mouse model ($TR\alpha_1$ loss-of-function). Notably, we discovered that under both normal and metabolically compromised conditions, T3-mediated increase in whole-body energy expenditure, in part, relies on $TR\alpha_1$ signaling in skeletal muscle. In contrast, T3-induced hyperthermia does not require functional $TR\alpha_1$ in skeletal muscle.

2 | MATERIALS AND METHODS

2.1 | Animals

A mouse line carrying a dominant negative mutation, L400R, in the AF-2 domain of thyroid receptor alpha 1 ($TR\alpha^{L400R}$); was generated as previously described.[9] This mutated version is not expressed in the absence of Cre recombination, since a LoxP-PGKNeoRPolyA-LoxP cassette is blocking its transcription. To selectively express the mutated receptor in skeletal muscle, a HSA-Cre mouse line was used. This line is used to drive Cre-recombinase in skeletal muscle tissue from E9 and onward, with no expression in heart, liver, and other tissues.[10] The expression of Cre-recombinase drives deletion of the PGKNeoRPolyA cassette and thereby allowing for transcription of $TR\alpha^{L400R}$ version of the receptor (Figure S1C).[9] $TR\alpha^{L400R\text{-}flox/flox}$ mice were crossed with HSA-Cre mice resulting in $TR\alpha^{L400R\ +/flox}$ HSA-Cre + (referred to as $TR\alpha^{HSACre}$) or $TR\alpha^{L400R\ +/flox}$ Cre negative littermates, which were used as controls (referred to as WT). In Figure 1H-K a mixture of $TR\alpha^{L400R\ +/flox}$ Cre negative and WT littermate-mice were used as controls (WT).

Male mice were maintained on a 12 hours dark-light cycle housed at 22°C or 30°C. Mice had free access to water and chow diet (Altromin 1324, Brogaarden, DK) or HFD containing 60E% fat (D12492; Research Diets). For ex vivo assessment of muscle and adipose tissue, mice were sacrificed by cervical dislocation, and SOL, EDL, BAT, and iWAT were excised and snap frozen in liquid nitrogen. Animal studies were approved by and conducted in accordance with the Danish Animal Experiments Inspectorate.

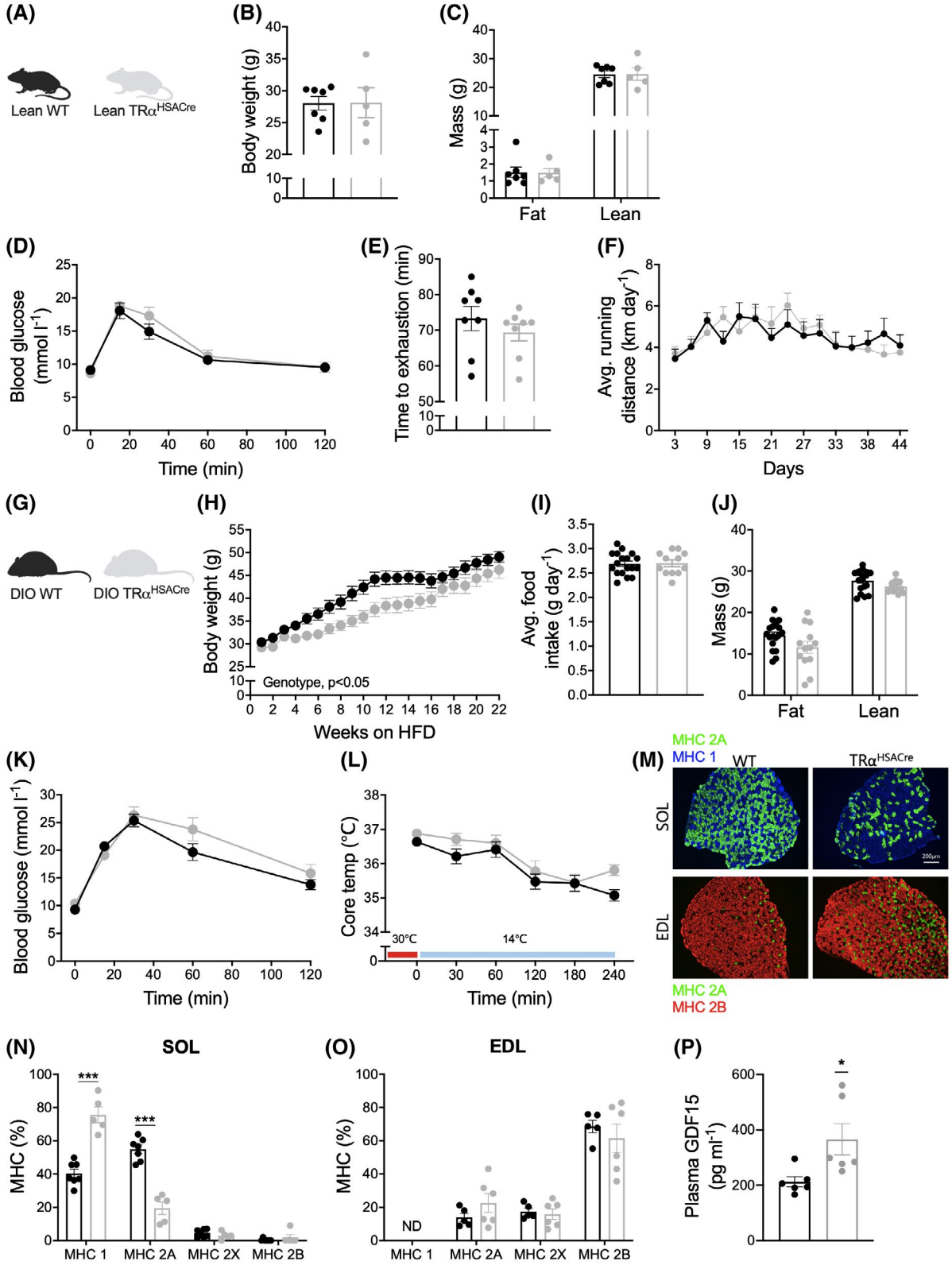

FIGURE 1 Skeletal muscle TRα$_1$ is crucial for muscle morphology but plays a minor role in energy and glucose metabolism. A, wild-type (WT) (black) and TRα^{HSACre} (gray) mice were characterized on a chow diet. B, body weight, (C) body composition, (D) glucose tolerance, (E) exercise capacity on a treadmill, and (F) average daily running distance during 44 days of voluntary wheel running (lean WT/TRα^{HSACre}, n = 7-8/5-10). G, another cohort of mice were exposed to high-fat diet-induced obesity (DIO), WT (black) and TRα^{HSACre} (gray). H, effects on body weight, (I) food intake, (J) body composition, and (K) glucose tolerance (DIO WT/TRα^{HSACre}, n = 18/12-13). L, core temperature at thermoneutrality and during a mild cold challenge (DIO WT/TRα^{HSACre}, n = 8/10). M, N, O, fiber-type distribution in SOL and EDL muscles, and (P) circulating GDF15 levels (DIO WT/TRα^{HSACre}, n = 5-7/5-6). Unpaired *t* test in B, C, E, I J, N, O, and P was applied to test for genotype differences, and a two-way ANOVA with a Bonferroni post hoc test in D, F, H, K, and L, was applied to evaluate the effects of genotype and time. Post hoc analyses were performed irrespective of ANOVA results. ***$P < .001$, *$P < .05$. All data are presented as mean ± SEM

2.2 | In vivo pharmacology and energy metabolism studies

T3 (Sigma-Aldrich) was administered subcutaneously (s.c.) at 100 nmol per kg body weight (5 μL per gram body weight) in agreement with previous work exploring whole-body energy expenditure in response to T3.[11] For chronic treatment studies, vehicle control or T3 was administered 1 hour before the onset of the dark cycle. The last injection was administered 2 hours before sacrifice and tissue harvest. Body composition was measured by magnetic resonance imaging (EchoMRI-4in1Tm, Echo Medical system LLC, USA). To determine energy expenditure, oxygen (O_2) consumption was measured by indirect calorimetry (TSE System, Germany). O_2 and carbon dioxide (CO_2) were measured every 10 minutes for 5 days. Mice were habituated to individual cages for 3 days prior to measurement. For the cold challenge, HFD-fed mice were acclimatized to thermoneutral housing before being exposed to an acute 6-hour moderate-cold challenge study, during which the mice were housed at 14°C. Body temperature was measured using a rectal probe (BIO-TK8851, Bioseblab, France).

2.3 | Glucose tolerance studies

For assessment of glucose tolerance, mice were fasted for 6 hours followed by an intraperitoneal challenge with either 1.75 g (HFD-fed mice) or 2 g (chow-fed mice) glucose per kg body weight. Glucose levels were measured in venous blood, sampled from the tail before (0 minute) and at 15, 30, 60, and 120 minutes post injection using a handheld glucometer (Contour XT, Bayer, CH).

2.4 | Exercise studies

2.4.1 | Voluntary running

Mice were acclimated to running wheels (23 cm in diameter, Techniplast, I) for 1 week after which running distance and time was measured for 6 weeks by a computer (Sigma Pure 1 Topline 2016, D) using a magnet affixed to the wheels.

2.4.2 | Treadmill-running

The week prior to the experimental test, mice were acclimated to the treadmill (Treadmill TSE Systems, Germany) on three separate days for 10 minutes at13.8 m/min at 0° incline. Mice were then exposed to an endurance running test starting with 10 minutes at 6 m/min then 40 minutes at 16.2 m/min (50% of max speed) with a slope at 10° followed by gradually increased speed (0.6 m/min) until exhaustion. Exhaustion was defined when mice fell back to the grid three times within 30 seconds. All tests were blinded in terms of genotype.

2.5 | Transcriptomic analysis by RNA sequencing

Total RNA was isolated using RNeasy mini kit (Qiagen) according to the manufacturers' protocol. Messenger RNA sequencing libraries were prepared using the Illumina TruSeq Stranded mRNA protocol (Illumina). Poly-A containing mRNAs were purified by poly-T attached magnetic beads, fragmented, and cDNA was synthesized using SuperScript III Reverse Transcriptase (Thermo Fisher Scientific). cDNA was adenylated to prime for adapter ligation and after a clean-up using AMPure beads (Beckman coulter), the DNA fragments were amplified using PCR followed by a final clean-up. Libraries were quality-controlled using a Bioanalyzer instrument (Agilent Technologies) and subjected to 51-bp paired-end sequencing on a NovaSeq 6000 (Illumina). A total of 1.07 billion reads were generated.

2.6 | Bioinformatic analysis

The STAR aligner[12] v. 2.7.3a was used to align RNA-seq read against the mm10 mouse genome assembly and GENCODE vM22 mouse transcripts.[13] The software program featureCounts v. 1.6.4 was used to summarize reads onto genes.[14] Testing for differential expression was performed using edgeR[4] v. 3.26.8 using the quasi-likelihood framework with a fitted model of the form *~0 + group* where *group* encoded both genotype and treatment.[15] Contrasts were constructed as described in the edgeR manual. Gene Ontology[5] enrichments were found using the CAMERA function[7] which is part of the edgeR package.[16,17] Only gene ontologies with between 5 and 500 genes were investigated.

2.7 | Quantitative real-time PCR

2.7.1 | RNA extraction & cDNA synthesis

Tissues (skeletal muscle and BAT) were quickly dissected and frozen either on dry ice or with liquid nitrogen and stored at −80°C. Tissues were homogenized in a TRIzol reagent (QIAzol Lysis Reagent, Qiagen) using a stainless steel bead (Qiagen) and a TissueLyser LT (Qiagen) for 3 minutes at 20 Hz. Then, 200 μL of chloroform (Sigma-Aldrich) was added and tubes were shaken vigorously for 15 seconds and left at RT for 2 minutes, followed by centrifugation at 4°C for 15 minutes at 12 000 *g*. The aqueous phase was mixed 1:1 with 70% ethanol and further processed using RNeasy

Lipid Tissue Mini Kit (Qiagen) following the instructions provided by the manufacturer. For muscle tissue, the lysis procedure described in the enclosed protocol in the Fibrous Tissue Mini Kit (Qiagen) was followed. After RNA extraction, RNA concentration and purity were measured using a NanoDrop 2000 (Thermo Fisher). A total of 500 ng of RNA (1000 ng RNA in the case of BAT) was converted into cDNA by mixing FS buffer and DTT (Thermo Fisher) with Random Primers (Sigma-Aldrich) and incubated for 3 minutes at 70°C. This was followed by the addition of dNTPs, RNase out, Superscript III (Thermo Fisher), and cDNA was synthesized in a thermal cycler using following steps: 5 minutes at 25°C, 60 minutes at 50°C, 15 minutes at 70°C. cDNA was diluted 1:100 in nuclease-free water and kept at −20°C until further processing.

2.7.2 | qPCR

SYBR green qPCR was performed using Precision plus qPCR Mastermix containing SYBR green (Primer Design, #PrecisionPLUS). For primer sequences, see Table S1. qPCR was performed in 384-well plates on a Light Cycler 480 Real-Time PCR machine using 2 minutes preincubation at 95°C followed by 45 cycles of 60 seconds at 60°C, and melting curves were performed by stepwise increasing the temperature from 60°C to 95°C. Quantification of mRNA expression was performed according to the delta-delta Ct method.

2.7.3 | Western blotting

BAT and iWAT were homogenized in ice-cold MG buffer (50mM HEPES, 150mM NaCl, 20mM $Na_4P_2O_7$, 20mM β-glycerophosphate, 10mM NaF, 2mM Na_3VO_4, 1mM EDTA, 1mM EGTA, 1% Nonidet P-40, 10% glycerol, 2mM PMSF, 10 µg/mL leupeptin, 10 µg/mL aprotinin, and 3mM benzamidine). Supernatant was collected after 20 minutes centrifugation at 16 000 *g* at 4°C and protein content was determined with the bicinchoninic acid method (BCA no. 23225, Pierce, US). Samples were heated to 96°C in Laemmli buffer and exposed to SDS-PAGE and semidry blotting. Polyacrylamide gels from each tissue were placed on the same membrane to ensure same transfer efficiency determined by quantification of standard (deviation ± 2). UCP1 antibody was from Abcam (1:7500, ab10983), and anti-rabbit polyclonal, horseradish peroxidase (HRP)-conjugated secondary antibody from Dako Cymation (1:5000). Chemiluminescent signals were detected (Bio-Rad ChemiDocTM MPImaging System), quantified (Image Lab version 4.0), and related to WT vehicle group.

2.8 | Mitochondrial respiratory capacity

To study the mitochondrial respiration in skeletal muscle, T3-treated and vehicle-treated mice were sacrificed by cervical dislocation. Muscles with different energy metabolism, SOL (oxidative) and EDL (glycolytic), were excised and stored in ice-cold relaxing buffer (BIOPS: K_2EGTA (100 mM), Na_2ATP (5.77 mM), $MgCl_2$ $6H_2O$ (6.56 mM), taurine (20 mM), Na_2Phospho-creatine (15 mM), imidazole (20 mM), dithiothreitol (0.5 mM), and MES (50 mM), pH = 7.1) and immediately analyzed for mitochondrial respiratory capacity. Mitochondrial respiratory capacity was measured in permeabilized skeletal muscle fibers using high-resolution respirometry (Oroboros Instruments, Innsbruck, Austria). The procedure has been described in detail elsewhere.[18] In brief, muscle fibers were dissected in ice-cold relaxing buffer (BIOPS) to a high level of fiber separation. Fibers were then placed in ice-cold BIOPS containing saponin (50 µg/mL) for 30 minutes to allow permeabilization of the outer cellular membrane.[19] The fibers where then washed twice for 10 minutes in MiR05 (sucrose (110 mM), potassium lactobionate (60 mM), EGTA (0.5 mM), $MgCl_2$ (3 mM), taurine (20 mM), KH_2PO_4 (10 mM), HEPES (20 mM), and BSA (1 g/l), pH 7.1) on ice. Approximately 2 mg was weighed and placed in each Oxygraph chamber. All measurements were carried out in MiR05 at 37°C after hyperoxygenation to avoid potential oxygen limitation. The following protocol was used in soleus and EDL: malate (2 mM), glutamate (10 mM), and pyruvate (5 mM) were added to determine state 2 respiration with complex I linked substrates (LEAK). ADP (5 mM) was added to evaluate state 3 respiration with complex I linked substrates (CI_P). Cytochrome *c* (10 µM) was added to control for outer mitochondrial membrane integrity. Finally, succinate (10 mM) was added to evaluate complex I + II-linked respiration ($CI + II_P$).

2.9 | Muscle morphology

SOL and EDL muscles were isolated and snap-frozen on dry ice and embedded in TissueTek and cut in 10 µm transverse sections on a cryostat. The sections were fixed using a mixture of acetone/100% alcohol (1:1) for 20 minutes. The sections were then preincubated in 5% normal donkey serum to block nonspecific binding. The mixture of primary antibodies (Developmental Studies Hybridoma Bank, University of Iowa): BA-D5 (IgG2b) specific for MyHC-I, SC-71 (IgG1) specific for MyHC-2A and BF-F3 (IgM) specific for MyHC-2B, was applied to detect the different myosin heavy chain isoforms. Type 2X fibers are not recognized by these antibodies and remain black. For immunofluorescence, the mixture of three different secondary

antibodies (Jackson ImmunoResearch): goat anti-mouse IgG1, conjugated with DyLight488 fluorophore (for SC-71); goat anti-mouse IgG2b, conjugated with DyLight405 fluorophore (for BA-D5); goat anti-mouse IgM, conjugated with DyLight549 fluorophore (for BF-F3) were used. After 1-hr incubation with secondary antibodies, sections were washed and embedded with Dako mounting media. Pictures were collected with an epifluorescence Olympus BX61microscope equipped with an Olympus DP71 camera. The relative number composition (%) of each muscle fiber type was analyzed using ImageJ software (NIH).

2.10 | Blood plasma analyses

Plasma levels of total T3 (DNOV053, NovaTec Immundiagnostica GmbH, Germany), total T4 (EIA-4568 DRG Diagnostics, Germany), and GDF15 (ELISA, R&D systems, catalog no. MGD150) were determined according to instructions provided by the manufacturer.

2.11 | Statistics

Statistical analyses were performed on data distributed in a normal pattern using one- or two-way ANOVA followed by Bonferroni's post hoc analysis as appropriate, or an unpaired two-tailed Student's *t* test. Post hoc analyses were performed irrespective of the two-way ANOVA results. All results are presented as mean ± SEM, and $P < .05$ was considered significant. Selection of differentially expressed genes and gene ontology enrichments were done based on false discovery adjusted P-values. Analyses were performed using Prism version 8 (GraphPad, US).

3 | RESULTS

3.1 | Skeletal muscle TRα$_1$ defines fiber-type composition in slow-twitch muscle but is largely dispensable for exercise capacity and energy homeostasis

To study the role of thyroid hormone receptor signaling in skeletal muscle on whole-body energy metabolism, we generated a skeletal muscle-specific TRα$_1$ loss-of-function mouse model (TRα^{HSACre}) (Figure S1A-C). No differences in body weight, fat and lean mass, or glucose tolerance were observed between genotypes (Figure 1B-D). Exhaustive running capacity on treadmill and voluntary wheel running, measured for 6 weeks, also were not different between genotypes (Figure 1E,F).

Another cohort of animals was fed a HFD for 22 weeks. We observed a slower weight gain trajectory for the TRα^{HSACre} mice relative to the WT mice in response to the dietary challenge (Figure 1H), which could not be explained by differences in food intake (Figure 1I). Following 18 weeks of HFD exposure, the TRα^{HSACre} mice weighed the same as the WT mice. No genotype differences in body composition, glucose tolerance, or body temperature in response to a moderate cold challenge (14°C for 4 hours) were found in the weight-matched HFD fed mice (Figure 1J-L). Notably, TRα^{HSACre} mice displayed an increase in type I fibers and a decrease in type IIA fibers in slow-twitch soleus muscle (SOL) compared to WT mice (Figure 1N). This difference, however, was not present in fast-twitch extensor digitorum longus (EDL) muscle (Figure 1O). The fiber-type switch in slow-twitch muscle was accompanied by an increase (72%) in circulating growth differentiation factor 15 (GDF15), a systemic marker of cellular and mitochondrial stress (Figure 1P).

3.2 | TRα$_1$ in skeletal muscle is required for T3-induced energy expenditure but is dispensable for T3-induced elevation in body temperature

To study the importance of skeletal muscle TRα$_1$ on thyroid hormone-induced energy expenditure, five different cohorts of TRα^{HSACre} and WT littermate mice were treated daily for either 5, 7,or 14 days with s.c. injections of T3 or vehicle. Plasma concentrations of T3 and T4 were similar between vehicle-treated lean and DIO TRα^{HSACre} and WT littermate controls (Figure 2A-C,F-H). As expected, T3 treatment resulted in increased T3 but decreased T4 plasma concentrations following 7 days of T3 (100 nmol/kg) treatment and with no differences between genotypes (Figure 2B,C,G,H). Indirect calorimetry revealed an increase in energy expenditure in response to T3 treatment in both lean and obese WT mice (Figure 2D,E,I,J, Figure S2A,B). T3 treatment did not significantly increase energy expenditure in lean TRα^{HSACre} mice (Figure 2D,E). In DIO WT mice the effect of T3 on metabolic rate was more pronounced than in lean WT mice suggesting that the thermogenic effect of T3 is related to fat mass. In this context, it may be that the absence of functional TRα$_1$ in muscle will have less impact on energy expenditure in DIO mice, than in a lean mouse. Accordingly, during the day, T3-mediated increase in metabolic rate was similar in WT and TRα^{HSACre} mice, whereas during dark phase, T3-mediated increase in energy expenditure was only observed in WT mice (Figure 2I,J). The consecutive increase in T3-stimulated energy expenditure in DIO mice is similar to what we have previously observed in this dietary model.[11]

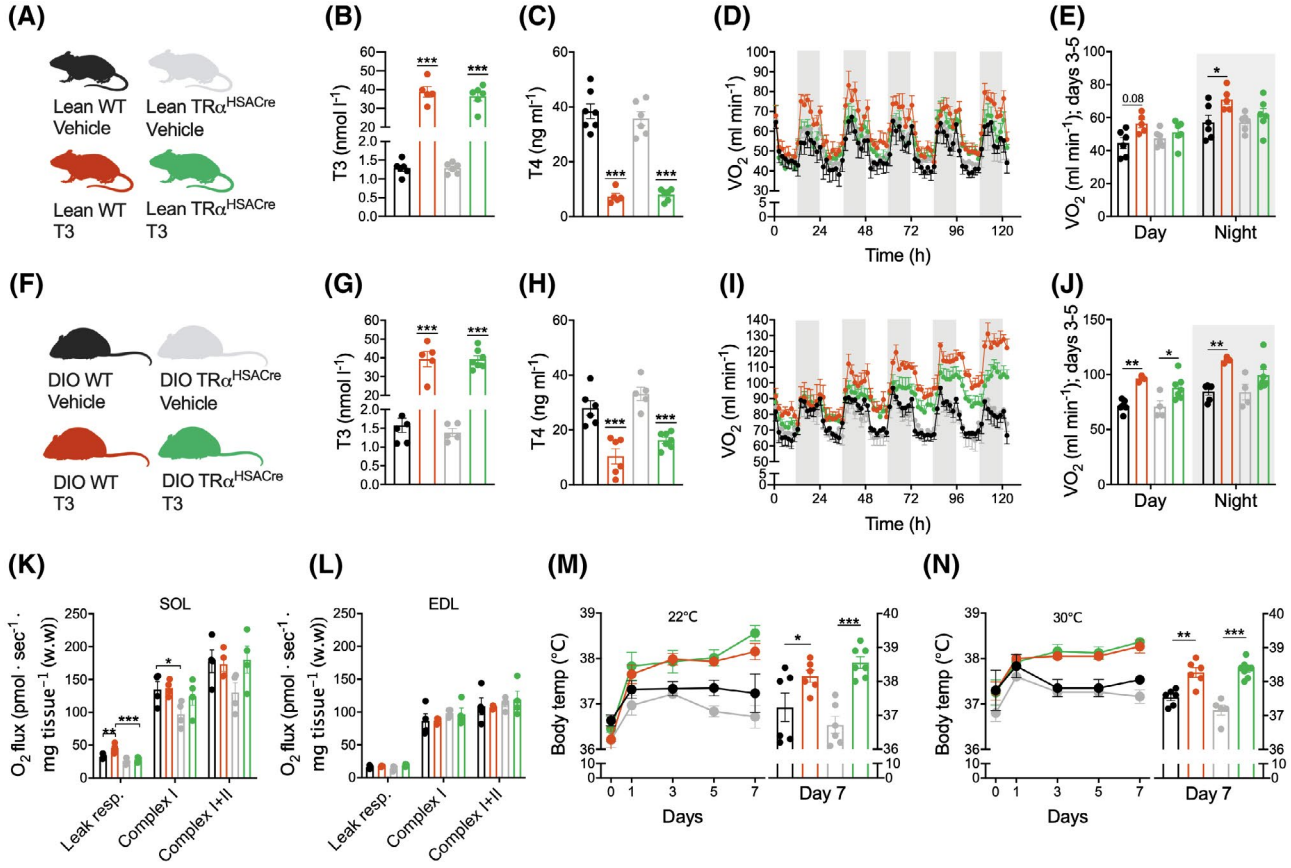

FIGURE 2 $TR\alpha_1$ in skeletal muscle is essential for T3-mediated increase in energy expenditure but is dispensable for T3-induced pyrexia. A, chow-fed lean WT and $TR\alpha^{HSACre}$ mice were injected daily (s.c.) with either vehicle (WT/$TR\alpha^{HSACre}$, n = 6/6) or T3 (100 nmol/kg) (WT/$TR\alpha^{HSACre}$, n = 6/6) for 5 days. B, plasma T3 and (C) T4 concentrations. D, effects on longitudinal energy expenditure and (E) energy expenditure quantified for days 3-5. F, DIO WT and $TR\alpha^{HSACre}$ mice were daily injected (s.c.) with either vehicle (WT/$TR\alpha^{HSACre}$, n = 6/4) or T3 (WT/$TR\alpha^{HSACre}$, n = 4/7) for 5 days. G, plasma T3 and (H) T4 concentrations. I, effects on longitudinal energy expenditure and (J) energy expenditure quantified for days 3-5. Chow-fed lean mice WT and $TR\alpha^{HSACre}$ mice were daily injected (s.c.) with either vehicle (WT/$TR\alpha^{HSACre}$, n = 4/4) or T3 (WT/$TR\alpha^{HSACre}$, n = 4/4) for 5 days. Ex vivo mitochondrial respiration in (K) SOL and (L) EDL muscles. DIO WT and $TR\alpha^{HSACre}$ mice were daily injected (s.c.) with either vehicle (WT/$TR\alpha^{HSACre}$, n = 6/6) or T3 (WT/$TR\alpha^{HSACre}$, n = 6/7) for 7 days. M, body temperature at room temperature and at (N) thermoneutral conditions. A one-way ANOVA with selected pairs (treatment vs. genotype) in K and L or a two-way ANOVA with a Bonferroni post hoc test in B, C, E G, H, J, M, and N was applied to evaluate differences in genotype and/or treatment. Post hoc analyses were performed irrespective of ANOVA results. $^*P < .05$, $^{**}P < .01$, $^{***}P < .001$. All data are presented as mean ± SEM

To decipher the muscle-specific effect of T3 on mitochondrial respiration in WT and $TR\alpha^{HSACre}$ mice, slow-twitch (SOL) and fast-twitch (EDL) muscles were excised from T3-treated mice and assessed for mitochondrial respiratory capacity (Figure 2K,L). In SOL, leak respiration (state 2) was similar between genotypes, but, in the context of T3 treatment, respiration only increased in WT mice, mirroring the whole-body indirect calorimetry data (Figure 2K). Oxidative phosphorylation capacity with complex I linked substrate revealed an impaired respiration in SOL in the non-stimulated state in $TR\alpha^{HSACre}$ mice relative to WT mice. Assessment of complex I- and complex I + II-linked respiration identified that T3 stimulation in $TR\alpha^{HSACre}$ raised respiration to an extent similar to that of WT mice. No differences in mitochondrial respiration were observed in EDL (Figure 2L).

The mechanisms by which thyroid hormones increase body temperature are elusive. To test a possible role for muscle $TR\alpha_1$ in T3-mediated elevation of body temperature, we measured core body temperature in WT and $TR\alpha^{HSACre}$ mice treated daily with either T3 or vehicle for 7 days. In agreement with previous studies, T3 treatment significantly elevated body temperature in WT mice at both ambient room temperature (22°C) and under thermoneutral conditions (30°C) (Figure 2M,N). Notably, $TR\alpha^{HSACre}$ mice treated with T3 responded similarly to WT mice treated with T3 in terms of body temperature increase at both 22°C and 30°C (Figure 2M,N). Furthermore, no compensatory differences in BAT weight or UCP1 protein expression in BAT and iWAT were observed in DIO $TR\alpha^{HSACre}$ mice relative to DIO WT mice in response to 14 days of T3 or vehicle treatment (Figure S2C-G). Together, these

findings suggest that 1) thyroid hormone signaling in skeletal muscle does not contribute to T3-induced pyrexia, and 2) thyroid hormone-mediated increase in energy expenditure and T3-induced pyrexia are not entirely interconnected processes.

3.3 | Structural and metabolic pathways dominate the transcriptome in response to T3-mediated activation of TRα$_1$ in soleus muscle

To dissect the mechanistic underpinnings of the muscle-linked induction in whole-body energy expenditure in response to T3 treatment, we performed RNA sequencing (RNA-seq) of WT and TRα^{HSACre} SOL from both treated and non-treated conditions. These analyses revealed that 788 transcripts were differentially expressed between WT SOL and TRα^{HSACre} SOL (Figure 3A). Under non-stimulated conditions, multiple genes linked to fiber-type composition and muscle morphology were differentially expressed in the TRα^{HSACre} mice compared with WT mice (Figure 3A). Furthermore, genes associated with muscle thermogenesis, such as sarcolipin and MSS51, were different between genotypes. In response to T3 treatment, expression profiling identified an enrichment of genes with the ontology terms "NADP biosynthesis" and "branched chain amino acids (BCAA) metabolism" to be differentially regulated in WT mice relative to TRα^{HSACre} mice (Figure 3B). Relative expression of top T3-responsive transcripts in SOL from WT mice in comparison to TRα^{HSACre} mice revealed a clear distinction in the transcriptional regulation (Figure 3C, Figure S3A). Notably, a clear transcriptional response in SOL to systemic T3 administration remained despite the mutation of TRα$_1$ in muscle. This might reflect systemic effects of T3 that subsequently introduce secondary effects on the muscle transcriptome. Assessment of key genes involved in muscle thermogenesis (Figure 3D) and muscle fiber-type morphology (Figure 3E) demonstrated differential expression between WT mice and TRα^{HSACre} mice in both non-stimulated and T3-induced conditions. Notably, the non-stimulated increase in sarcolipin mRNA in the TRα^{HSACre} mice was also evident in EDL, gastrocnemius, and quadriceps muscles (Figure S3B). Markers associated with BAT thermogenesis and thyroid hormone signaling in BAT were examined to determine the specificity of the TRα$_1$-related muscle transcriptional changes (Figure 3E). Whereas T3 clearly impacts transcripts involved in BAT thermogenesis, no differential expression between TRα^{HSACre} mice relative to WT mice was observed, implying that the muscle-specific mutation has no systemic "spill-over" to metabolic programs in other thermogenic tissues (Figure 3F).

4 | DISCUSSION

The coordinated biological mechanisms by which thyroid hormones regulate energy metabolism have been studied for more than 100 years. Yet, the key regulatory pathways remain elusive. Here, we use a skeletal muscle-specific TRα$_1$ loss-of-function mouse model to show that T3-mediated increase in whole-body energy expenditure, in part, relies on thyroid hormone-induced actions in skeletal muscle. Furthermore, we demonstrate that mechanisms independent of TRα$_1$ in skeletal muscle govern the increase in body temperature following T3 treatment. Our data support a model by which thyroid hormone actions in skeletal muscle promote metabolic rate via coordinated regulation of fiber-type composition, substrate metabolism, and muscle thermogenesis.

It is well established that thyroid hormones impact muscle fiber-type characteristics and mitochondrial activity.[20,21] Thyroid hormone excess induces a shift toward fast-twitch muscle fiber type,[22] whereas hypothyroidism leads to slow-twitch muscle phenotype.[23] The effects of thyroid hormones on muscle are considered to be mediated almost exclusively by TRα$_1$.[24,25] A recent study convincingly confirmed this using in vivo HA-tag insertions and antibodies for HA-tagged versions of TRα$_1$, TRα$_2$ and TRβ.[8] They demonstrated—at the protein level—that TRα$_1$ is the predominant thyroid hormone receptor in skeletal muscle. Functionally, this is supported by global thyroid hormone receptor KO studies showing that deletion of TRα$_1$ leads to a lower abundance of fast-twitch fibers in SOL and that ablation of TRβ has no consequences on muscle morphology.[26] Here we expand this knowledge by showing that muscle TRα$_1$ is necessary for maintaining normal fiber-type distribution. Although loss-of-function of TRα$_1$ in muscle dramatically impacts fiber-type composition in slow-twitch muscle, this morphological change does not affect exercise capacity or voluntary running.

To our surprise, metabolic rate was unperturbed in the TRα^{HSACre} mice under non-stimulated conditions at ambient temperature, and the ability of the TRα^{HSACre} mice to defend body temperature against mild cold stress was also intact. In comparison, global TRα KO mice have been reported to be cold intolerant and protected from diet-induced obesity.[27] Important to note, TRα is widely expressed throughout the body and global TRα KO mice suffer from a series of abnormalities, including abnormalities in brain development and in cardiac function.[28] The data presented here suggest that TRα$_1$ in skeletal muscle is dispensable for body temperature protection against mild cold stress. Conversely, muscle TRα$_1$ seems to play a minor role in the progression of diet-induced obesity. Here, we employed transcriptomics to identify molecular signals in muscle that could underlie the preserved metabolic rate in the TRα^{HSACre} mice. Notably, sarcolipin expression was

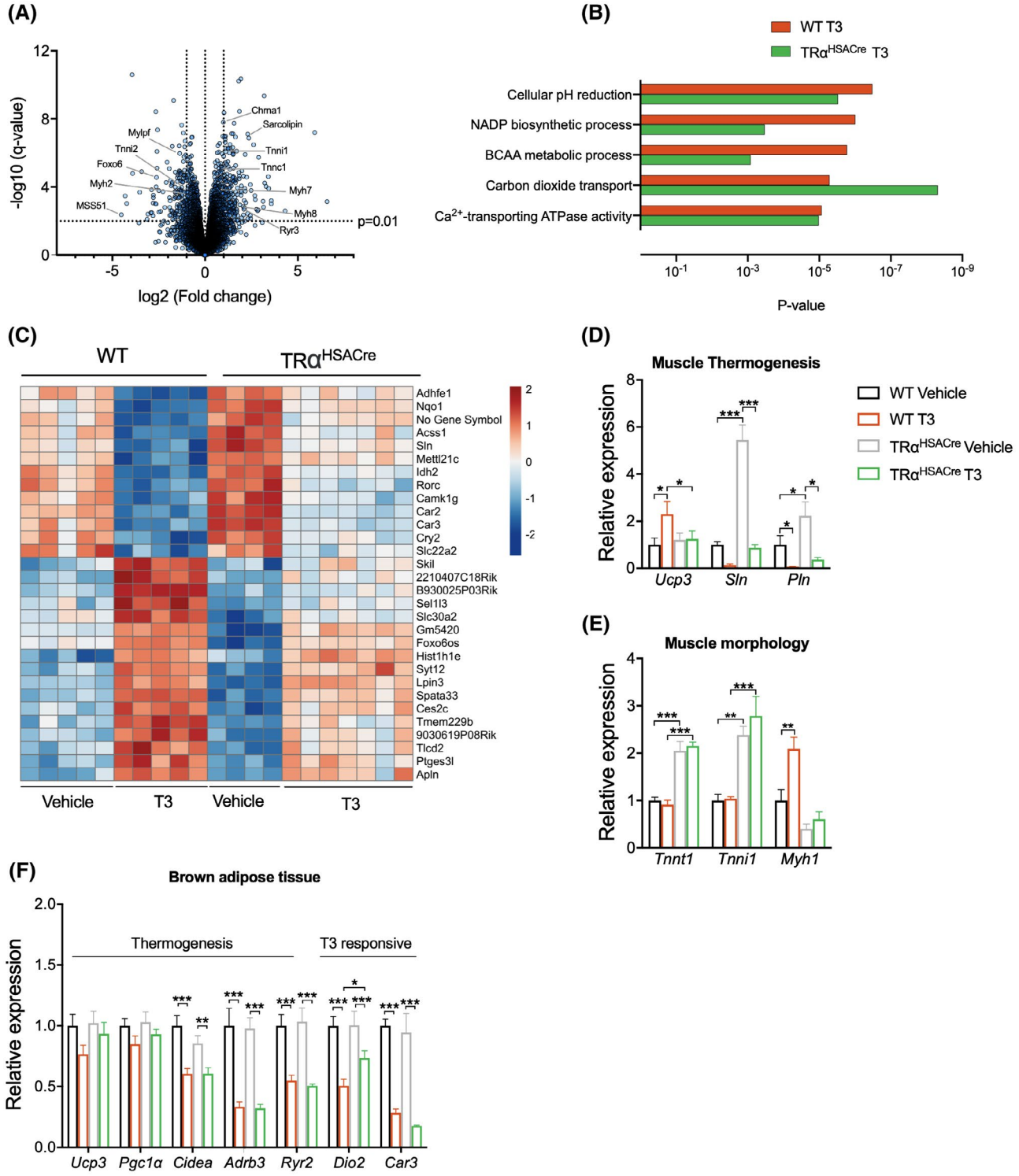

FIGURE 3 Transcriptome of T3-stimulated TRα$_1$ in soleus muscle. Volcano plot comparing the FDR-adjusted p-values (q-values) and fold change of the TRα^{HSACre} SOL transcriptome relative to WT SOL transcriptome under non-stimulated conditions. A, mice were injected daily (s.c.) with vehicle (WT/TRα^{HSACre}, n = 5-6/4-6) or T3 (WT/TRα^{HSACre}, n = 5-6/7) for 7 days. B, selected enriched Gene Ontologies that were significantly enriched in T3-treated soleus from WT mice compared to T3-treated SOL from TRα^{HSACre} mice. C, heatmap showing top regulated transcripts in WT T3-treated SOL and TRα^{HSACre} T3-treated SOL. Confirmatory qPCR analyses of transcripts involved in (D) muscle thermogenesis, (E) muscle morphology, and (F) BAT thermogenesis and thyroid hormone action. A one-way ANOVA with selected pairs (treatment vs genotype) with a Bonferroni post hoc test was applied to evaluate differences in genotype and/or treatment. Post hoc analyses were performed irrespective of ANOVA results. *$P < .05$, **$P < .01$, ***$P < .001$. All data are presented as mean ± SEM

increased >5-fold in TRα^{HSACre} mice in the non-stimulated state. Sarcolipin modulates muscle thermogenesis via uncoupling of SERCA-mediated ATP hydrolysis.[29] Parallel ablation of sarcolipin and BAT thermogenic capacity renders mice cold intolerant, and reintroduction of sarcolipin expression in skeletal muscle rescues the phenotype.[30,31] Corroborating an interdependence between BAT and muscle for non-shivering thermogenesis, UCP1 KO mice increase muscle sarcolipin levels in the cold.[32] Thus, the pronounced increase in sarcolipin expression in TRα^{HSACre} skeletal muscle might represent a compensatory mechanism in the context of impaired thyroid signaling in muscle[33] and suggests a hitherto unrecognized interdependence or crosstalk between thyroid and sarcolipin-mediated signaling and control of muscle thermogenesis.

The most striking observation in the present study is that T3-mediated increase in energy expenditure is partly dependent on muscle TRα_1 signaling. This is perhaps surprising given the increased focus on thyroid hormones and BAT thermogenesis over the last decade, yet, it aligns with recent studies showing that thyroid thermogenesis is intact in UCP1 KO mice.[6,7] Here, we demonstrate that T3-mediated elevation in whole-body energy expenditure can be ascribed, in part, to actions in muscle. Because the indirect calorimetry studies of the present study were executed at ambient temperature (22°C), a partially retained thermogenic capacity in BAT might contribute to the quantity of muscle-independent thermogenesis observed in the T3-treated TRα^{HSACre} mice. Furthermore, futile substrate cycling in other tissues, for example, liver, likely contributes to the increase in whole-body energy expenditure in response to exogenous T3.[11]

Another key finding of the present work is that the T3-mediated increase in energy expenditure is partially dissociated from T3-induced defense of an elevated body temperature. Accordingly, we show that TRα_1 signaling in muscle is not required for T3-induced pyrexia, suggesting that thyroid hormone-mediated increase in body temperature is governed by other organs. A segregation of energy expenditure and body temperature in response to tissue-specific thyroid hormone signaling has been observed previously. A pharmacological study reported that a glucagon-T3 hybrid molecule signals in hepatocytes and adipocytes to increase energy expenditure, without affecting body temperature.[11] Given that BAT weight and UCP1 protein expression in adipose tissues were similar between T3-treated TRα^{HSACre} and WT mice, it suggests that fat thermogenesis is not engaged to compensate for the ablated TRα signaling in skeletal muscle. However, we cannot exclude other compensatory mechanism such as regulation of tail heat dissipation. Hence, future studies are warranted to untangle the molecular interconnectedness between energy expenditure and body temperature, and assessment of heat loss from the tail surface, in response to pharmacological T3, should be considered in such studies.[34]

In conclusion, we demonstrate that skeletal muscle is a key site for thyroid hormone-mediated increase in energy expenditure. Furthermore, we reveal that TRα_1 in skeletal muscle is dispensable for T3-governed induction in body temperature, and, therefore, that thyroid hormone-induced energy expenditure is partially disconnected from T3-induced pyrexia. Our data also show that TRα_1 is fundamental for muscle fiber-type composition and, in the absence of TRα_1 signaling, molecular compensatory mechanisms appear to safeguard the metabolic rate. As such, the present study supports a repositioning of skeletal muscle as a crucial target organ for thyroid hormones in energy metabolism.

ACKNOWLEDGMENTS

A.-M. Lundsgaard, J. Lund, and A. M. Fritzen were supported by a research grant from the Danish Diabetes Academy, which is funded by the Novo Nordisk Foundation, grant number NNF17SA0031406. Furthermore, A. M. Fritzen was supported by the Alfred Benzon Foundation. O. Dmytriyeva is supported by the Danish Council for Independent Research (7016-00389A) granted to Prof. Thue W. Schwartz, who we thank for his generous support of the project. C. Clemmensen is supported by research grants from the Lundbeck Foundation (Fellowship R238-2016-2859) and the Novo Nordisk Foundation (grant number NNF17OC0026114). The authors thank the Single-Cell Omics Platform at CBMR for supporting the project. Novo Nordisk Foundation Center for Basic Metabolic Research is an independent Research Center, based at the University of Copenhagen, Denmark, and partially funded by an unconditional donation from the Novo Nordisk Foundation (www.cbmr.ku.dk) (Grant number NNF18CC0034900).

CONFLICT OF INTEREST

The authors declare that they have no conflict of interest.

AUTHOR CONTRIBUTION

T.S. Nicolaisen, A.B. Klein, and C. Clemmensen planned and designed the experiments. A.B. Klein and T.S. Nicolaisen carried out in vivo experiments with help from A.M. Fritzen, C.S. Carl, and A.-M. Lundsgaard. Assessment of mitochondrial respiratory capacity in skeletal muscles was done by S. Larsen, M. Frost, and O. Dmytriyeva performed skeletal muscle immunohistochemistry. C. Clemmensen, A.B. Klein, T.S. Nicolaisen, L.R. Ingerslev, and J. Lund analyzed and interpreted data. T. Ma, P. Schjerling, Z. Gerhart-Hines, F. Flamant, K. Gauthier, E.A. Richter and B. Kiens interpreted data. T.S. Nicolaisen, A.B. Klein, and C. Clemmensen wrote the manuscript, and all co-authors contributed to the final version of the manuscript.

DATA AVAILABILITY STATEMENT

The raw sequencing data and aligned read counts generated as part of this study has been deposited to the NCBI Sequence Read Archive. Accession number: GSE146336; https://www.ncbi.nlm.nih.gov/geo/query/acc.cgi?acc=GSE146336. The scripts used for the analysis of the sequencing data and figure generation are available at https://github.com/lars-worksund/GSE146336.

REFERENCES

1. Mullur R, Liu YY, Brent GA. Thyroid hormone regulation of metabolism. *Physiol Rev*. 2014;94:355-382.
2. Silva JE. Thermogenic mechanisms and their hormonal regulation. *Physiol Rev*. 2006;86:435-464.
3. Silva JE, Larsen PR. Adrenergic activation of triiodothyronine production in brown adipose tissue. *Nature*. 1983;305:712-713.
4. Silva JE, Larsen PR. Potential of brown adipose tissue type II thyroxine 5′-deiodinase as a local and systemic source of triiodothyronine in rats. *J Clin Invest*. 1985;76:2296-2305.
5. Lopez M, Varela L, Vazquez MJ, et al. Hypothalamic AMPK and fatty acid metabolism mediate thyroid regulation of energy balance. *Nat Med*. 2010;16:1001-1008.
6. Johann K, Cremer AL, Fischer AW, et al. Thyroid-hormone-induced browning of white adipose tissue does not contribute to thermogenesis and glucose consumption. *Cell Rep*. 2019;27:3385-3400.e3.
7. Dittner C, Lindsund E, Cannon B, Nedergaard J. At thermoneutrality, acute thyroxine-induced thermogenesis and pyrexia are independent of UCP1. *Mol Metab*. 2019;25:20-34.
8. Minakhina S, Bansal S, Zhang A, et al. A direct comparison of thyroid hormone receptor protein levels in mice provides unexpected insights into thyroid hormone action. *Thyroid*. 2020;30(8):1193-1204.
9. Quignodon L, Vincent S, Winter H, Samarut J, Flamant F. A point mutation in the activation function 2 domain of thyroid hormone receptor alpha1 expressed after CRE-mediated recombination partially recapitulates hypothyroidism. *Mol Endocrinol*. 2007;21:2350-2360.
10. Miniou P, Tiziano D, Frugier T, Roblot N, Le Meur M, Melki J. Gene targeting restricted to mouse striated muscle lineage. *Nucleic Acids Res*. 1999;27:e27.
11. Finan B, Clemmensen C, Zhu Z, et al. Chemical hybridization of glucagon and thyroid hormone optimizes therapeutic impact for metabolic disease. *Cell*. 2016;167:843-857.e14.
12. Dobin A, Davis CA, Schlesinger F, et al. STAR: ultrafast universal RNA-seq aligner. *Bioinformatics*. 2013;29:15-21.
13. Frankish A, Diekhans M, Ferreira AM, et al. GENCODE reference annotation for the human and mouse genomes. *Nucleic Acids Res*. 2019;47:D766-D773.
14. Liao Y, Smyth GK, Shi W. featureCounts: an efficient general purpose program for assigning sequence reads to genomic features. *Bioinformatics*. 2014;30:923-930.
15. Robinson MD, McCarthy DJ, Smyth GK. edgeR: a Bioconductor package for differential expression analysis of digital gene expression data. *Bioinformatics*. 2010;26:139-140.
16. The Gene Ontology, C. The gene ontology resource: 20 years and still going strong. *Nucleic Acids Res*. 2019;47:D330-D338.
17. Wu D, Smyth GK. Camera: a competitive gene set test accounting for inter-gene correlation. *Nucleic Acids Res*. 2012;40:e133.
18. Boushel R, Gnaiger E, Schjerling P, Skovbro M, Kraunsoe R, Dela F. Patients with type 2 diabetes have normal mitochondrial function in skeletal muscle. *Diabetologia*. 2007;50:790-796.
19. Kuznetsov AV, Veksler V, Gellerich FN, Saks V, Margreiter R, Kunz WS. Analysis of mitochondrial function in situ in permeabilized muscle fibers, tissues and cells. *Nat Protoc*. 2008;3:965-976.
20. Argov Z, Renshaw PF, Boden B, Winokur A, Bank WJ. Effects of thyroid hormones on skeletal muscle bioenergetics. In vivo phosphorus-31 magnetic resonance spectroscopy study of humans and rats. *J Clin Invest*. 1988;81:1695-1701.
21. Bloise FF, Cordeiro A, Ortiga-Carvalho TM. Role of thyroid hormone in skeletal muscle physiology. *J Endocrinol*. 2018;236:R57-R68.
22. Simonides WS, van Hardeveld C. Thyroid hormone as a determinant of metabolic and contractile phenotype of skeletal muscle. *Thyroid*. 2008;18:205-216.
23. Caiozzo VJ, Haddad F, Baker M, McCue S, Baldwin KM. MHC polymorphism in rodent plantaris muscle: effects of mechanical overload and hypothyroidism. *Am J Physiol Cell Physiol*. 2000;278:C709-C717.
24. Miyabara EH, Aoki MS, Soares AG, et al. Thyroid hormone receptor-beta-selective agonist GC-24 spares skeletal muscle type I to II fiber shift. *Cell Tissue Res*. 2005;321:233-241.
25. Salvatore D, Simonides WS, Dentice M, Zavacki AM, Larsen PR. Thyroid hormones and skeletal muscle—new insights and potential implications. *Nat Rev Endocrinol*. 2014;10:206-214.
26. Yu F, Gothe S, Wikstrom L, Forrest D, Vennstrom B, Larsson L. Effects of thyroid hormone receptor gene disruption on myosin isoform expression in mouse skeletal muscles. *Am J Physiol Regul Integr Comp Physiol*. 2000;278:R1545-R1554.
27. Pelletier P, Gauthier K, Sideleva O, Samarut J, Silva JE. Mice lacking the thyroid hormone receptor-alpha gene spend more energy in thermogenesis, burn more fat, and are less sensitive to high-fat diet-induced obesity. *Endocrinology*. 2008;149:6471-6486.
28. Flamant F, Samarut J. Thyroid hormone receptors: lessons from knockout and knock-in mutant mice. *Trends Endocrinol Metab*. 2003;14:85-90.
29. Smith WS, Broadbridge R, East JM, Lee AG. Sarcolipin uncouples hydrolysis of ATP from accumulation of Ca2+ by the Ca2+-ATPase of skeletal-muscle sarcoplasmic reticulum. *Biochem J*. 2002;361:277-286.
30. Rowland LA, Bal NC, Kozak LP, Periasamy M. Uncoupling protein 1 and sarcolipin are required to maintain optimal thermogenesis, and loss of both systems compromises survival of mice under cold stress. *J Biol Chem*. 2015;290:12282-12289.
31. Bal NC, Maurya SK, Sopariwala DH, et al. Sarcolipin is a newly identified regulator of muscle-based thermogenesis in mammals. *Nat Med*. 2012;18:1575-1579.
32. Bal NC, Singh S, Reis FCG, et al. Both brown adipose tissue and skeletal muscle thermogenesis processes are activated during mild to severe cold adaptation in mice. *J Biol Chem*. 2017;292:16616-16625.
33. Maurya SK, Bal NC, Sopariwala DH, et al. Sarcolipin is a key determinant of the basal metabolic rate, and its overexpression enhances energy expenditure and resistance against diet-induced obesity. *J Biol Chem*. 2015;290:10840-10849.

34. Warner A, Rahman A, Solsjo P, et al. Inappropriate heat dissipation ignites brown fat thermogenesis in mice with a mutant thyroid hormone receptor alpha1. *Proc Natl Acad Sci U S A*. 2013;110:16241-16246.

SUPPORTING INFORMATION

Additional Supporting Information may be found online in the Supporting Information section.

How to cite this article: Nicolaisen TS, Klein AB, Dmytriyeva O, et al. Thyroid hormone receptor α in skeletal muscle is essential for T3-mediated increase in energy expenditure. *The FASEB Journal*. 2020;34:15480–15491. https://doi.org/10.1096/fj.202001258RR